Structural Monitoring and Maintenance, *Vol. 10, No. 4 (2023) 315-337*
https://doi.org/10.12989/smm.2023.10.4.315

Investigation of the behavior of an RC beam strengthened by external bonding of a porous P-FGM and E-FGM plate in terms of interface stresses

Zahira Sadoun[1,2], Riadh Bennai[*1,2], Mokhtar Nebab[2,3], Mouloud Dahmane[4] and Hassen Ait Atmane[1,2]

[1]*Department of Civil Engineering, Faculty of Civil Engineering and Architecture, University Hassiba Benbouali of Chlef, Algeria*
[2]*Laboratory of Structures, Geotechnics and Risks, Department of Civil Engineering, Hassiba Benbouali University of Chlef, Algeria*
[3]*Department of Civil Engineering, Faculty of Sciences, University of M'Hamed BOUGARA Boumerdes, Algeria*
[4]*Department of planning and hydraulic engineering, Higher National School of Hydraulics, Blida 9000, Algeria*

(*Received November 5, 2023, Revised December 16, 2023, Accepted December 18, 2023*)

Abstract. During the design phase, it is crucial to determine the interface stresses between the reinforcing plate and the concrete base in order to predict plate end separation failures. In this work, a simple theoretical study of interface shear stresses in beams reinforced with P-FGM and E-FGM plates subjected to an arbitrarily positioned point load, or two symmetrical point loads, was presented using the linear elastic theory. The presence of pores in the reinforcing plate distributed in several forms was also taken into account. For this purpose, we analyze the effects of porosity and its distribution shape on the interracial normal and shear stresses of an FGM beam reinforced with an FRP plate under different types of load. Comparisons of the proposed model with existing analytical solutions in the literature confirm the feasibility and accuracy of this new approach. The influence of different parameters on the interfacial behavior of reinforced concrete beams reinforced with functionally graded porous plates is further examined in this parametric study using the proposed model. From the results obtained in this study, we can say that interface stress is significantly affected by several factors, including the pores present in the reinforcing plate and their distribution shape. Additionally, we can conclude from this study that reinforcement systems with composite plates are very effective in improving the flexural response of reinforced RC beams.

Keywords: FGM plate; interfacial stresses; normal stress; porosity; RC beams; shear stress; strengthening

1. Introduction

The lifespan of concrete structures such as bridges depends essentially on the satisfactory design and use of suitable construction materials. Failure of these factors may cause early structural degradation and deterioration, and replacing these structures is generally an expensive

*Corresponding author, Associate Professor, E-mail: r.bennai@yahoo.fr

 ISSN: 2288-6605 (Print), 2288-6613 (Online)

solution. The only way to keep the structure operating safely is to reinforce or renovate it. Consequently, an accurate understanding of the material and selected strengthening techniques is required for the strengthening of inadequate buildings (Aslam *et al*. 2015).

Many different techniques have been used to enhance structures in various ways. One of them is the use of composite materials, which have great mechanical properties, to retrofit reinforced concrete structures (Danraka *et al.* 2017). Strengthening wood, steel, or reinforced concrete beams by bonding composite plates has been found to be an effective technique to increase their load capacities (Van Pham 2021). It is generally accepted that the plate end debonding of the soffit plate from the concrete beam, which largely depends on the interfacial shear and normal stress concentration at the cut-off points of the plate, is one of the significant failure mechanisms in such a retrofitted beam (Guenaneche and Tounsi 2014).

Many researches have been done to predict the interfacial stresses, either analytically, numerically, or both; for instance, Smith and Teng (2001) proposed theoretical solutions for the interfacial shear and normal stresses in beams reinforced with FRP plate. A basic approximation on the fine elements of the interfaces in the beam of the armed forces behind a Soviet plaque collected presented by Teng *et al.* (2002) Afin d'évaluer la précision des analytiques approximatives actuelles de firme. For a simply supporting concrete beam that is externally bonded with a FRP plate, Tounsi and Benyoucef (2007) gives an improved theoretical interfacial stress that accounts for the adherents' shear deformations by assuming a linear shear stress over their thickness. Daouadji *et al.* (2008) presented a theoretical investigation to analyze the interfacial stresses in damaged RC beams externally bonded with FRP plate, taking into consideration the effect of the fiber orientations. Benachour *et al*. (2008) used the linear elastic theory and took into account the variation in the fiber orientation of the FRP plate to develop a solution for the interfacial normal and shear stress in simply supported beams strengthened with bonded prestressed FRP plates and subjected to a uniformly distributed load, an arbitrarily placed single point load, or two symmetric point loads. Mohamed *et al*. (2009) presented a theoretical interfacial stress analysis by including the creep and shrinkage effect and the interface slip effect for simply supported RC beams with a thin FRP composite plate. In the same context, Ameur *et al.* (2009) used linear elastic theory to evaluate the interfacial stress problem in steel beams reinforced with composite laminates bonded by hygrothermal aging. Interfacial stresses in clad beams exposed to arbitrary mechanical and thermal loads positioned symmetrically around mid-span were analyzed by a new analytical solution, according to Yang *et al.* (2009). In order to predict the interfacial stresses for simply supported, straight plated beams that were subjected to uniform distribution, Zhang and Teng (2010) developed a finite element approach. The five models' predictions are compared with one another and with analytical approaches of varying degrees of sophistication.

In the current theoretical work, the shear stresses of the adherends have been taken into account by assuming a parabolic distribution of shear stress over their thickness. Fahsi *et al*. (2011) investigated the effect of time-dependent deformations (shrinkage and creep) on the interfacial stresses between an RC beam and FRP plate. Recently, Daouadji (2013) proposed a theoretical approach to predicting the interfacial stresses in the adhesive layer of damaged RC beams repaired with externally bonded CFRP plate considering the shear deformations of the adherend by assuming a linear distribution of shear stress throughout the depth of the reinforced concrete beam. Bouchikhi *et al.* (2013) have investigated the effect of mixed adhesive joints (MAJs) and tapering plate on the interfacial stress distribution in the adhesive layer. The interfacial stress in simply supported steel beams reinforced with a bonded FRP plate and subjected to thermomechanical loadings was solved using a closed-form method by Benyoucef *et al*. (2014). To assess the

interfacial stresses in an I-beam of steel reinforced with bonded, hygrothermally aged CFRP plate, Bouakaz *et al.* (2014) developed a finite-element model using the commercial Abaqus software. In order to predict the interfacial stress of prestressed CFRP composite plate reinforced simply supported RC beams, Rabahi *et al*. (2016) developed an enhanced analytical and numerical approach. Daouadji et al. (2016) presented the results of an analytical and numerical solution for interfacial stresses in carbon fiber reinforced plastic (CFRP)–reinforced concrete (RC) hybrid beams studied by the finite element method. Du *et al*. (2016) proposed a new theoretical solution based on Timoshenko beam theory. The coupled governing differential equations of interfacial stresses are solved by the weighted residual method based on the least squares principle. The impact of shear deformation on both normal and shear stresses at the interface was measured at the same time using simple interfacial stress formulas. An interfacial stress study was provided by Daouadji *et al*. (2016) for a simply supported concrete beam that was reinforced with an FGM plate. Rabia *et al.* (2018) utilizing the theory of linear elasticity, were able to come up with a closed-form rigorous solution for the interfacial shear stress in simply supported beams that were strengthened with bonded prestressed E-FGM plates, the beams were also subjected to either a single point load that was arbitrarily positioned or two point loads that were symmetric. A theoretical method for predicting the interfacial strains in the adhesive layer of reinforced concrete beams that are reinforced with porous FRP plate was illustrated by Rabia et al. (2020). A new, modified rule of combination covering the porosity phases is used to incorporate the influence caused by porosity. The current theoretical investigations have considered the adherend shear deformations by assuming a linear shear stress over the thickness of the adherends. In their study, Liu and Dawood (2018) used a shear-lag formulation to analyze the elastic-plastic behavior of beams reinforced with externally attached fiber reinforced polymer (FRP) plates; the reinforcement was achieved utilizing ductile adhesives. The model possesses the capability to assess mechanical and thermal loading circumstances of any nature and provide solutions in closed-form for shearing and peeling scenarios. Du *et al*. (2019), proposed an improved analytical model for the stress analysis of an adhesive layer in a plated beam. Shan and Su (2020) proposed a new theoretical method on the adhesive stress concentration at the plate ends based on the Timoshenko beam theory, and two improved uncoupled governing equations for normal and shear stresses were proposed. Sha and Davidson (2020) analyzed the interfacial stresses in concrete beams strengthened by externally bonded FRP laminates subjected to UDL based on composite beam theory and taking into account the bond-slip relationship between FRP laminates and concrete. Long *et al.* (2020) developed a precise analytical solution for the interfacial stresses and overall stiffness of plated beams using the two-parameter elastic foundation model and the conventional Euler-Bernoulli beam model, they also demonstrated the effects of the interface and plate characteristics. Raza *et al*. (2021) examined the structural performance of recycled aggregate concrete columns repaired and reinforced with GFRP bars and spirals. FRP coating is effective for the renovation of RC columns that have suffered damage, both in the presence of low to medium pre-existing damage but also in heavily damaged columns (e.g., Sami *et al*. 2022, Berradia *et al*. 2022). In recent years, He *et al*. (2023) presented a new hybrid reinforcement method, for which reinforced concrete (RC) beams are reinforced in flexure by external bonding of a steel plate of variable thickness and a pocket FRP with end anchor. Al-Bukhaiti *et al*. (2023) proposed a model using artificial neural networks for the prediction of interface bond strength between CFRP layers and reinforced concrete. Experimental and numerical studies on the structural behavior of RCRBs reinforced with durable materials are presented by Hamoda *et al*. (2023). Mohamed *et al*. (2023) studied the structural behavior of deep beams with openings an experimentally and analytically.

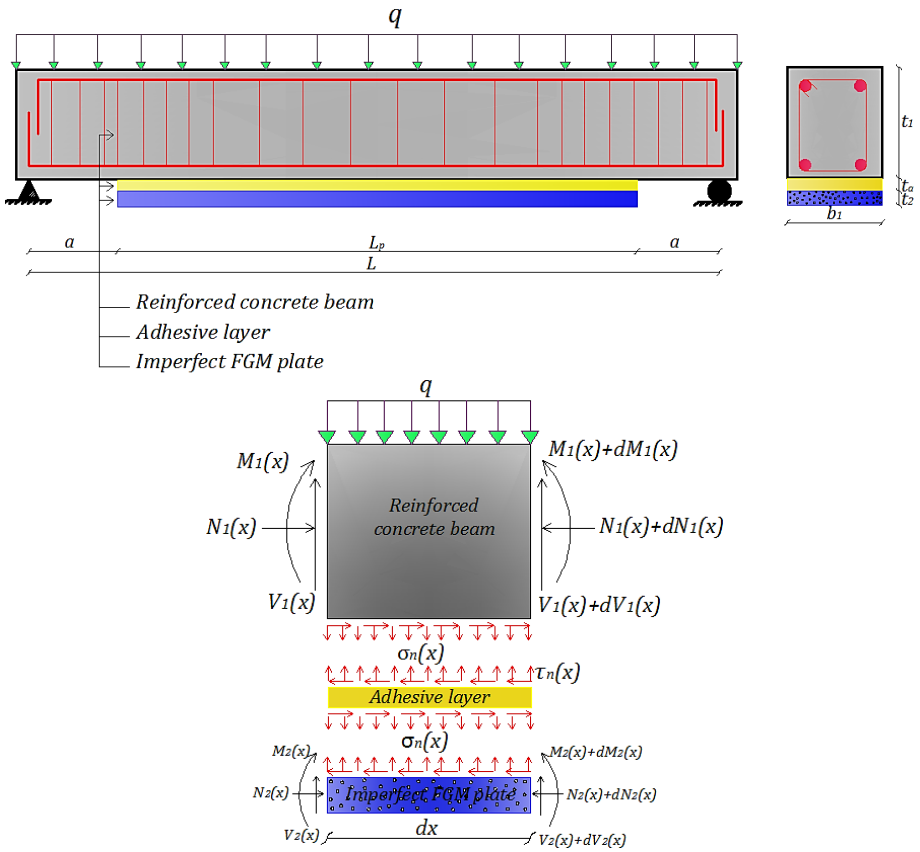

Fig. 1 Simply supported beam strengthened with bonded FGM plate

An experimental study of the flexural response of reinforced concrete beams externally bonded with hybrid laminates (FRP) made of carbon fibers and polyethylene terephthalate was proposed by Yu-Lei *et al*. (2024).

Functionally graded material (FGM), a new kind of composite material that has excellent mechanical properties, a high degree of environmental adaptability, and a strong designability, has drawn considerable interest from academics. The functionally graded material has several potential applications and is being employed extensively in the domains of aerospace, mechanical, nuclear, and other technological fields Zhang *et al*. (2023). FGM were created by gradually mixing two or more components. Additive manufacturing can be used successfully to manufacture FGM (Bennai *et al.* 2022, Mellal *et al.* 2023, Kim *et al.* 2023). Due to technical difficulties during the manufacturing of FGMs with two different porosity distributions, namely, even and uneven distribution, the FGM plates contain porosity (Wang *et al.* 2017, Ayache *et al*. 2018, Bennai *et al.* 2019a, Bennai *et al.* 2019 b, Nebab *et al*. 2019, Ait Atmane *et al.* 2021, Mellal *et al.* 2021).

The objective of this study is to propose a general analytical model to predict the distribution of interfacial shear and normal stresses of a concrete beam reinforced with FGM porous plates under different types of mechanical loading. Different forms of porosity distribution at the level of the reinforcing plates were taken into account in this study. Additionally, the plate is assumed to be

composed of two materials with different phases across the thickness, based on a volume fraction based on power (P-FGM) and exponential (E-FGM) functions. Assuming that the shear stresses are linearly distributed across the bond thickness, the bond shear strains were included in the theoretical analyses. Comparison with the most recent results in the literature was used to validate the current model. A parametric study is carried out to show the effect of the porosity, the geometric and the material parameters on the interfacial stresses. Finally, numerical comparisons between the current new solution and the previous solutions provide for an obvious comprehension of the impacts of different factors. The current results should be of interest to civil and structural engineering researchers, as well as civil engineers.

2. Analytical approach

2.1 Basic assumptions

The analytical approach is based on the following assumptions (Daouadji *et al.* 2016)

a. The concrete, adhesive, and FGM materials behave elastically and linearly.
b. No slip is permitted at the interface of the bond (i.e., the adhesive–concrete interface and the adhesive– FGM plate interface have a perfect bond).
c. The adhesive is assumed to only function is to transfer stresses from the concrete to the composite plate reinforcement.
d. The stresses are constant across the thickness of the adhesive layer.

Since the functionally graded materials is an orthotropic material. In analytical study (Daouadji *et al.* 2016) classical plate theory is used to determine the stress and strain behaviors of the externally bonded composite plate to predict the whole mechanical performance of the composite – strengthened structure.

2.2 Properties of the FGMs constituent materials

In order to create the FGMs, two materials are combined whose properties vary continuously along the thickness direction in accordance with some mathematical functions with respect to a particular volume fraction index. Most researchers describe the volume fractions using a power-law function or an exponential function. On the other hand, very few studies used the sigmoid function to characterize the volume fractions.

In this research, we take into account an imperfect FGM (porous) plate with a volume fraction of porosity and a different type of metal and ceramic distribution.

i. Porosities unevenly distributed for P-FGM:

$$E(z) = E_m + (E_c - E_m).\left(0.5 + \frac{z}{h}\right)^N - (E_c - E_m).\Omega.\left(1 - \frac{2.|z|}{h}\right) \tag{1}$$

The mechanical characteristics of the porous plate are supposed to vary according to a well-defined law depending on the distribution of porosity. In the following, four porosity distributions in the thickness direction are considered (linear, logarithmic, exponential and sinus), as shown in Table 1.

Table 1 The uneven porosity distribution function Ω

Sources	distribution shape	Ω
Wattanasakulpong and Ungbhakorn (2014)	Linear	$\frac{\zeta_1}{2}$
Gupta and Talha (2017)	Logarithmic	$\log\left(1+\frac{\zeta_1}{2}\right)$
Ayache *et al*. (2018)	Exponentially	$1-e^{-\frac{\zeta_1}{2}}$
Ait Atmane *et al*. (2021)	Sinus	$0.325.\sin\left(\frac{3.\zeta_1}{2}\right)$

ii. Porosities unevenly distributed for E-FGM

$$E(z)=E_m.\exp\left(\ln\left(\frac{E_c}{E_m}\right).\left(\frac{z}{h}+\frac{1}{2}\right)^N-\frac{2.\zeta_1}{1-\zeta_1}\right) \tag{2}$$

In which subscripts c and m represent ceramic and metal, respectively. In addition, N is a power-law index that defines the material variation characterization through the height of the plate. The Poisson's coefficient v is considered constant. ζ_1 is the porosity coefficient ($\zeta_1 << 1$). ζ_1 =0 indicates the non-porous functionally graded plate.

The linear constitutive relations of an FG plate can be written as

$$\begin{Bmatrix}\sigma_x\\ \sigma_y\\ \tau_{yz}\\ \tau_{xz}\\ \tau_{xy}\end{Bmatrix}=\begin{bmatrix}Q_{11} & Q_{12} & 0 & 0 & 0\\ Q_{12} & Q_{22} & 0 & 0 & 0\\ 0 & 0 & Q_{44} & 0 & 0\\ 0 & 0 & 0 & Q_{55} & 0\\ 0 & 0 & 0 & 0 & Q_{66}\end{bmatrix}\begin{Bmatrix}\varepsilon_x\\ \varepsilon_y\\ \gamma_{yz}\\ \gamma_{xz}\\ \gamma_{xy}\end{Bmatrix} \tag{3}$$

Where $(\sigma_x,\sigma_y,\tau_{yz},\tau_{xz},\tau_{xy})$ and $(\varepsilon_x,\varepsilon_y,\gamma_{yz},\gamma_{xz},\gamma_{xy})$ are the stress and strain components respectively. The computation of the elastic constants Q_{ij} in the plane stress reduced elastic constants, defined as

$$Q_{11}=Q_{22}=\frac{E(z)}{1-\upsilon^2};\qquad Q_{12}=\frac{\upsilon\,E(z)}{1-\upsilon^2} \tag{4}$$

Where A_{ij} and D_{ij} are the plate stiffness, defined by

$$A_{ij}=\int_{-h/2}^{h/2}Q_{ij}dz \qquad\qquad D_{ij}=\int_{-h/2}^{h/2}Q_{ij}z^2dz \tag{5}$$

Where $A_{11}^{'}$ and $D_{11}^{'}$ are defined as

$$A_{11}^{'} = \frac{A_{22}}{A_{11}A_{22} - A_{12}^2} \qquad D_{11}^{'} = \frac{D_{22}}{D_{11}D_{22} - D_{12}^2} \tag{6}$$

$A_{11}^{'}$: Is the first term of the inverse matrix $\left[A_{ij}^{'}\right]$ of the extensional matrix $\left[A_{ij}\right]$

$D_{11}^{'}$ **:** Is the first term of the inverse matrix $\left[D_{ij}^{'}\right]$ of the flexural matrix $\left[D_{ij}\right]$

2.3 Distribution of shear stress along the FGM – concrete interface plate

According to their respective expressions, the strains in the RC beam near the adhesive interface and the external FGM reinforcement (Daouadji *et al*. 2016) are as follows

$$\varepsilon_1(x) = \frac{du_1(x)}{dx} = \frac{y_1}{E_1 I_1} M_1(x) + \frac{N_1(x)}{E_1 A_1} + \frac{t_1}{4G_1}\frac{d\tau_a}{dx} \tag{7}$$

$$\varepsilon_2(x) = \frac{du_2(x)}{dx} = \frac{-y_2}{E_2 I_2} M_2(x) + \frac{N_2(x)}{E_2 A_2} - \frac{5t_2}{12G_2}\frac{d\tau_a}{dx} \tag{8}$$

The following is an expression for the shear stress in the adhesive

$$\tau_a = \tau(x) = K_s\left[u_2(x) - u_1(x)\right] \tag{9}$$

Where $K_s = G_a / t_a$ is the shear stiffness of the adhesive, G_a and t_a are the shear modulud and thickness of the adhesive, respectively, and $u_1(x)$ and $u_2(x)$ are the longitudinal displacements at the base of adherend 1 and the top of adherend 2.

Differentiating Eqs. (9) the above expression, we obtain

$$\frac{d\tau(x)}{dx} = K_s\left[\frac{du_2(x)}{dx} - \frac{du_1(x)}{dx}\right] \tag{10}$$

The equilibrum of the RC beam and FGM plate leads to the following relationships (Daouadjin *et al*. 2016). Consideration of horizontal equilibrium gives

$$\frac{dN_1(x)}{dx} = -b_2\tau(x) \tag{11}$$

$$\frac{dN_2(x)}{dx} = b_2\tau(x) \tag{12}$$

Where, b_2 is the width of the FGM plate. Assuming equal curvature in the beam and the FGM plate, the relationship between the moments in the two adherends can be expressed as

$$M_1(x) = RM_2(x) \tag{13}$$

with

$$R = \frac{E_1 I_1 D_{11}^{'}}{b_2} \tag{14}$$

Moment equilibrium of the differential segment of the plated beam in Fig. 1 gives

$$M_T(x) = M_1(x) + M_2(x) + N(x)\left(y_1 + t_a + \frac{t_2}{2}\right) \tag{15}$$

where $M_T(x)$ is the total applied moment.

As a function of the interfacial shear stress and the total applied moment, the bending moment in each adherend is expressed as follows

$$M_1(x) = \frac{R}{R+1}\left[M_T(x) - b_2\int_0^x \tau(x)\left(y_1 + t_a + \frac{t_2}{2}\right)dx\right] \tag{16}$$

$$M_2(x) = \frac{1}{R+1}\left[M_T(x) - b_2\int_0^x \tau(x)\left(y_1 + t_a + \frac{t_2}{2}\right)dx\right] \tag{17}$$

The first derivative of the bending moment in each adherend gives

$$\frac{dM_1(x)}{dx} = \frac{R}{R+1}\left[V_T(x) - b_2\tau(x)(y_1 + t_a + \frac{t_2}{2}\right] \tag{18}$$

$$\frac{dM_2(x)}{dx} = \frac{1}{R+1}\left[V_T(x) - b_2\tau(x)(y_1 + t_a + \frac{t_2}{2}\right] \tag{19}$$

Substituting Equations Eqs. (7) and (8) into Eqs. (10) and differentiating the resulting equation yields

$$\frac{d^2\tau(x)}{dx^2} = K_s\left(\frac{A_{11}^{'}}{b_2}\frac{dN_2(x)}{dx} - D_{11}^{'}\frac{t_2}{\mathbf{2}b_2}\frac{dM_2(x)}{dx} - \frac{y_1}{E_1 I_1}\frac{dM_1(x)}{dx} + \frac{\mathbf{1}}{E_1 A_1}\frac{dN_1(x)}{dx} - \frac{t_1}{\mathbf{4}G_1}\frac{d^2\tau_a}{dx^2}\right) \tag{20}$$

Substitutiog Eqs. (18), (19) and Esq. (11), (12) into Eq. (19) gives the following governing differential equation for the interfacial shear stress

$$\frac{d^2\tau(x)}{dx^2} - K_1\left(A_{11}^{'} + \frac{b_2}{E_1 A_1} + \frac{(y_1 + t_2/2)(y_1 + t_a + t_2/2)}{E_1 I_1 D_{11}^{'} + b_2}b_2 D_{11}^{'}\right)\tau(x) + K_1\left(\frac{(y_1 + t_2/2)}{E_1 I_1 D_{11}^{'} + b_2}D_{11}^{'}\right)V_T(x) = 0 \tag{21}$$

$$\text{where}: K_1 = \frac{1}{\left(\frac{t_a}{G_a} + \frac{t_1}{4G_1}\right)} \tag{22}$$

In order to keep things simple, the general solutions provided below are only applicable to loading that is either concentrated or uniformly distributed over part of the beam's entire span, or both.

For such loading $d^2V_T(x)/dx^2 = \mathbf{0}$ and the general solution to Eq. (20) presented by

$$\tau(x) = B_1 cosh(\lambda x) + B_2 sinh(\lambda x) + m_1 V_T(x) \tag{23}$$

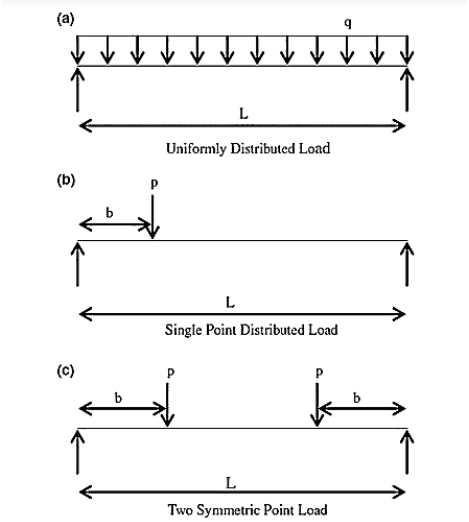

Fig. 2 Load cases

where

$$\lambda^2 = K_1\left(A_{11}^{'} + \frac{b_2}{E_1A_1} + \frac{(y_1 + t_2/2)(y_1 + t_a + t_2/2)}{E_1I_1D_{11}^{'} + b_2}b_2D_{11}^{'}\right) \tag{24}$$

$$m_1 = \frac{K_1}{\lambda^2}\left(\frac{(y_1 + t_2/2)}{E_1I_1D_{11}^{'} + b_2}D_{11}^{'}\right) \tag{25}$$

and B_1 and B_1 are the constant coefficients determined from the boundary conditions.

In this study, a simply supported beam was investigated, which is subjected to a uniformly distributed load, a single point load and two symmetric point loads Fig. 2.

i. Interfacial shear stress for a uniformly distributed load

The general solution for the interfacial shear stress for this load case is

$$\tau(x) = \left[\frac{m_2a}{2}(L-a) - m_1\right]\frac{qe^{-\lambda x}}{\lambda} + m_1q\left(\frac{L}{2} - a - x\right) \qquad 0 \le x \le L_P \tag{26}$$

Where q is the uniformly distributed load and x; a; L and L_p are defined in Fig. 1.

ii Interfacial shear stress for a single point load

The general solution for the interfacial shear stress for this load case is

$$a < b: \quad \tau(x) = \begin{cases} \frac{m_2}{\lambda}Pa\left(1 - \frac{b}{L}\right)e^{-\lambda x} + m_1P\left(1 - \frac{b}{L}\right) - m_1P\cosh(\lambda x)e^{-k} & 0 \le x \le (b-a) \\ \frac{m_2}{\lambda}Pa\left(1 - \frac{b}{L}\right)e^{-\lambda x} - m_1\frac{Pb}{L} + m_1P\sinh(k)e^{-\lambda x} & (b-a) \le x \le L_p \end{cases} \tag{27}$$

$$a > b: \quad \tau(x) = \frac{m_2}{\lambda} Pb\left(1 - \frac{a}{L}\right)e^{-\lambda x} - m_1 \frac{Pb}{L} \qquad 0 \le x \le L_P \tag{28}$$

iii Interfacial shear stress for two points loads

The general solution for the interfacial shear stress for this load case is

$$a < b: \quad \tau(x) = \begin{cases} \frac{m_2}{\lambda} Pae^{-\lambda x} + m_1 P - m_1 P \cosh(\lambda x)e^{-k} & 0 \le x \le (b-a) \\ \frac{m_2}{\lambda} Pae^{-\lambda x} + m_1 P \sinh(k)e^{-\lambda x} & (b-a) \le x \le \frac{L_p}{2} \end{cases} \tag{29}$$

$$a > b: \quad \tau(x) = \frac{m_2}{\lambda} Pbe^{-\lambda x} \qquad 0 \le x \le L_P \tag{30}$$

2.4 Distribution of normal stress along the FGM – concrete interface plate

The following is an expression for the interfacial normal stress in the adhesive:

$$\sigma_n(x) = K_n \Delta w(x) = K_n \left[w_2(x) - w_1(x) \right] \tag{31}$$

Where K_n is the normal stiffness of the adhesive per unit length and can be written as

$$K_n = \frac{E_a}{t_a} \tag{32}$$

$w_1(x)$ and $w_1(x)$ are the normal displacements of adherends 1 and 2 respectively

Differentiating Eq. (31) twice results in

$$\frac{d^2\sigma_n(x)}{dx^2} = K_n \left[\frac{d^2 w_2(x)}{dx^2} - \frac{d^2 w_1(x)}{dx^2} \right] \tag{33}$$

Considering the moment–curvature relationships for the beam and the external reinforcement, respectively, gives

$$\frac{d^2 w_1(x)}{dx^2} = -\frac{M_1(x)}{E_1 I_1} \text{ and } \frac{d^2 w_2(x)}{dx^2} = -\frac{D_{11}' M_1(x)}{E_2 I_2} \tag{34}$$

The equilibrium of adherends 1 and 2, leads to the following relationships

$$\text{Adherend 1:} \quad \frac{dM_1(x)}{dx} = V_1(x) - b_2 y_1 \tau(x) \text{ and } \frac{dV_1(x)}{dx} = -b_2 \sigma_n(x) - q \tag{35}$$

$$\text{Adherend 2:} \quad \frac{dM_2(x)}{dx} = V_2(x) - b_2 \frac{t_2}{2} \tau(x) \text{ and } \frac{dV_2(x)}{dx} = -b_2 \sigma_n(x) \tag{36}$$

Based on the above equilibrium equations, the governing differential equations for the deflection of adherends 1 and 2, expressed in terms of the interfacial shear and normal stresses, are given as follows

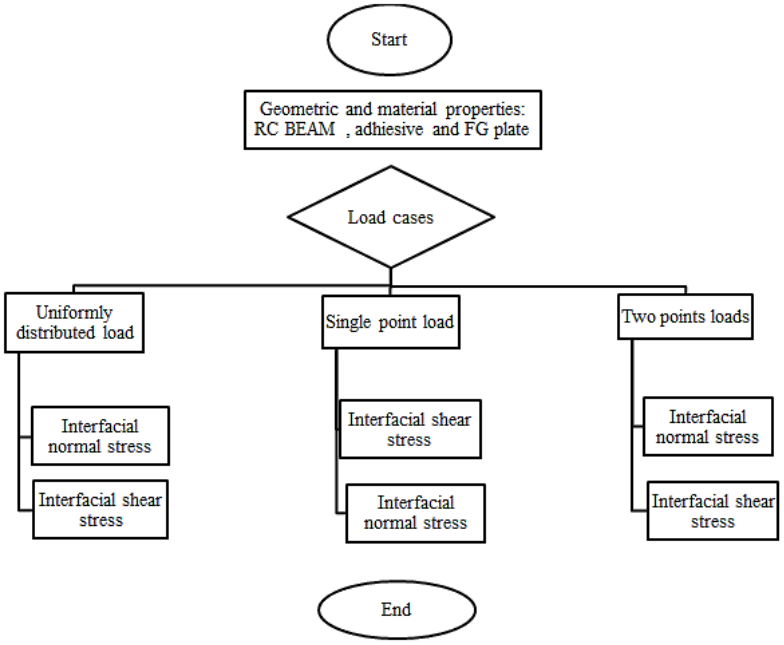

Fig. 3 Flowchart of the computation of normal and shear stresses for single loads, double loads, and uniform loads

$$Adherend\,1: \quad \frac{d^4 w_1(x)}{dx^4} = \frac{1}{E_1 I_1} b_2 \sigma_n(x) + \frac{y_1}{E_1 I_1} b_2 \frac{d\tau(x)}{dx} + \frac{q}{E_1 I_1} \tag{37}$$

$$Adherend\,2: \quad \frac{d^4 w_2(x)}{dx^4} = -D_{11}^{'} \sigma_n(x) + D_{11}^{'} \frac{t_2}{2} \frac{d\tau(x)}{dx} \tag{38}$$

Substituting both Eqs. (37), (38) into the fourth derivation of the interfacial normal stress obtainable from Eq. (31) gives the following governing differential equation for the interfacial normal stress

$$\frac{d^4 \sigma_n(x)}{dx^4} + K_n \left(D_{11}^{'} + \frac{b_2}{E_1 I_1} \right) \sigma_n(x) - K_n \left(D_{11}^{'} \frac{t_2}{2} - \frac{y_1 b_2}{E_1 I_1} \right) \frac{d\tau(x)}{dx} + \frac{q K_n}{E_1 I_1} = 0 \tag{39}$$

Fourth-order differential Eq. (39) has the following general solution

$$\sigma_n(x) = e^{-\beta x} \left[C_1 \cos(\beta x) + C_2 \sin(\beta x) \right] + e^{\beta x} \left[C_3 \cos(\beta x) + C_4 \sin(\beta x) \right] - n_1 \frac{d\tau(x)}{dx} - n_2 q \tag{40}$$

For large values of x it is assumed that the normal stress approaches zero and as a result, $C_3 = C_4 = 0$. The general solution becomes

$$\sigma_n(x) = e^{-\beta x} \left[C_1 \cos(\beta x) + C_2 \sin(\beta x) \right] - n_1 \frac{d\tau(x)}{dx} - n_2 q \tag{41}$$

$$\beta = \sqrt[4]{\frac{K_n}{4}}\left(D_{11}^{'} + \frac{b_2}{E_1 I_1} \right) \tag{42}$$

$$n_1 = \left(\frac{y_1 b_2 - D_{11}^{'} E_1 I_1 t_2 / 2}{D_{11}^{'} E_1 I_1 + b_2} \right) \qquad n_2 = \left(\frac{1}{D_{11}^{'} E_1 I_1 + b_2} \right) \tag{43}$$

The constants C_1 and C_2 in Eq. (40) are determined using the boundary conditions and are written as follows, as given by (Daouadji *et al*. 2016)

$$C_1 = \frac{K_n}{2\beta^3 E_1 I_1}\left[V_T(0) + \beta M_T(0) \right] - \frac{n_3}{2\beta^3}\tau(0) + \frac{n_1}{2\beta^3}\left(\frac{d^4\tau(0)}{dx^4} + \beta \frac{d^3\tau(0)}{dx^3} \right) \tag{44}$$

$$C_2 = -\frac{K_n}{2\beta^2 E_1 I_1} M_T(0) - \frac{n_1}{2\beta^2}\frac{d^3\tau(0)}{dx^3} \tag{45}$$

$$n_3 = b_2 K_n \left(\frac{y_1}{E_1 I_1} - \frac{D_{11}^{'} t_2}{2b_2} \right) \tag{46}$$

The working methodology in this study is a flowchart of the calculation of normal and shear stresses for single loads, double loads, and uniform loads.

3. Results and discussion

In this section, two cases are investigated. In the first, a comparison between the results of the present model and those in the literature is presented, where the effects of porosity are taken into account. In the next section, a parametric analysis is carried out to better understand the effects of different parameters on the distribution of interfacial stresses.

3.1 Geometric and material properties

The material used for the present studies is an RC beam bonded with an imperfect FGM plate, with a glass or carbon fiber reinforced plastic (GFRP or CFRP) or with a steel plate. The beam is simply supported and subjected to a different type of loading (a uniformly distributed load, a single point distributed load and a two symmetrical point load). A summary of the geometric and material properties is given in Table 2. The span of RC beam is L = 3000 mm, the distance from the support to the end of the plate is a = 300 mm, the mid-point load is 150 *KN* and UDL is 50 *KN*/*m*.

3.2 Validation of results

In this section, the interfacial shear and normal stresses from the various closed-form solutions that already exist and the current solution are compared. For the RC beam strengthened by bonding CFRP, GFRP, steel plate, P-FGM or E-FGM, the results of the peak interfacial shear and normal stresses (at the end of the soffit plate) are shown in Table 3. Fig. 3 plots the interfacial shear and normal stress near the plate end for the example RC beam bonded with a P-FGM plate for the uniformly distributed load case. The results show that the peak interfacial stresses

Table 2 Geometric and material properties

component	Width (mm)	Depth (mm)	Young's modulus (MPa)	Poisson's ratio	Shear modulus (MPa)
RC beam	b_1=200	t_1=300	E_1=30000	0.18	/
Adhesive layer	b_a=200	t_a=2	E_a=3000	0.35	/
GFRP	b_2=200	t_2=4	E_2=50000	0.28	G_{12}=5000
CFRP	b_2=200	t_2=4	E_2=140000	0.28	G_{12}=5000
Steel plate	b_2=200	t_2=4	E_2=200000	0.3	
FGM(AL_2O_3)	b_2=200	t_2=4	E_c=380000 E_m=70000	0.3	G_{12}=5000
FGM(Zr O_2)	b_2=200	t_2=4	E_c=200000 E_m=70000	/	G_{12}=5000

Table 3 Comparison of peak interfacial shear and normal stresses (MPa)

RC Beam with	Model	Uniformly Distributed Load		Mid-point load		Two point load	
		$\tau(MPa)$	$\sigma(MPa)$	$\tau(MPa)$	$\sigma(MPa)$	$\tau(MPa)$	$\sigma(MPa)$
CFRP	Tounsi *et al.* (2006)	1.791	1.078	2.051	1.234	-	-
	Rabahi *et al.* (2018)	1.812	1.0893	2.074	1.246	2.718	1.590
	Present Model	1.998	1.188	2.278	1.347	4.556	2.962
GFRP	Tounsi *et al.* (2006)	1.085	0.826	1.228	0.935		
	Rabahi *et al.* (2018)	1.093	0.832	1.236	0.942	1.733	1.290
	Present Model	1.217	0.914	1.374	1.030	2.748	2.218
Steel plate	Tounsi *et al.* (2006)	2.120	1.175	2.438	1.350	-	-
	Rabahi *et al.* (2018)	2.126	1.176	2.445	1.352	3.126	1.680
	Present Model	2.355	1.280	2.674	1.454	5.348	3.232
P-FGM	Rabahi *et al.* (2018) (AL_2O_3)	1.826	1.060	2.090	1.213	2.737	1.543
	Present Model(AL_2O_3)	2.071	1.158	2.364	1.311	4.728	2.932
	Present Model (ZrO_2)	1.712	1.063	1.945	1.201	3.890	2.646
E-FGM	Present Model (AL_2O_3)	1.587	1.009	1.800	1.139	3.600	2.508
	Present Model (ZrO_2)	0.952	1.370	1.550	1.073	3.101	2.335

calculated by the present theory are higher than those provided by(Tounsi 2006) and (Rabahi *et al.* 2018). This means that the distribution of adhesive interfacial stresses is significantly influenced by adherend shear deformation.

3.3 Parametric study

In this section, a parametric study is carried out to better understand the effects of several parameters on the distributions of the interfacial stresses in an undamaged RC beam bonded with an imperfect (porous) FGM plate. The beams are simply supported and subjected to a uniformly distributed load. A summary of the geometric and material properties is given in Table 1. The span of the RC beam is 3000 mm, the distance from the support to the end of the plate is 300 mm and the uniformly distributed load is 50 *KN*/*m*.

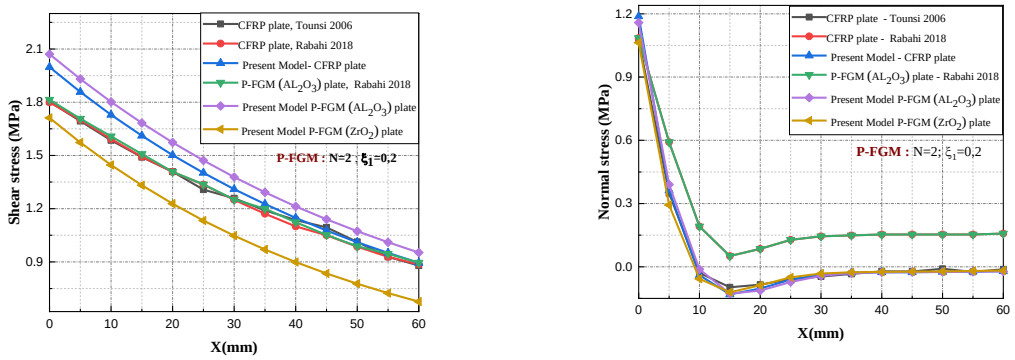

(a) (b)

Fig. 4 Comparison of interfacial shear and normal stress for P-FGM plated RC beam with the analytical results

Table 4 Effect of the porosity on the interfacial stresses of the RC beam strengthened with a porous FGM plate under uniform distributed load

Shear stress , P-FGM , N=10				
ζ1	Uneven porosity distribution functions			
	Linear	Logarithmic	exponential	Sinus
0	1.694	1.694	1.694	1.694
0.1	1.598	1.601	1.601	1.601
0.2	1.494	1.505	1505	1.503
0.3	1.381	1.405	1.406	1.401
Normal stress, P-FGM, N=10				
ζ1	Uneven porosity distribution functions			
	Linear	Logarithmic	exponential	Sinus
0	1.022	1.022	1.022	1.02
0.1	0.974	0.975	0.975	0.975
0.2	0.919	0.924	0.925	0.924
0.3	0.858	0.71	0.87	0.869

3.3.1 Porosity effect on the interfacial stresses

The study of the effect of the porosity on the interfacial shear and normal stresses of the RC beam strengthened with a porous P-FGM plate under uniformly distributed load (UDL) (Table 4 and Fig. 5), where the degree of homogeneity of the P-FGM is set N = 10. The volume fraction of porosity is considered equal to (0, 0.1.0.2 and 0.3) and the distribution functions of porosity in the P-FGM plate are also tested (Linear function, Logarithmic function, exponential function and Sinus function).

It is clear from the results presented in Table 4 and Fig. 5 that the interracial shear stresses decrease with increasing FG plate porosity parameter. We can explain this by decreasing plate stiffness due to higher porosity. In addition, it is very remarkable that the maximum stress values are obtained for the case of a pore distribution in exponential form.

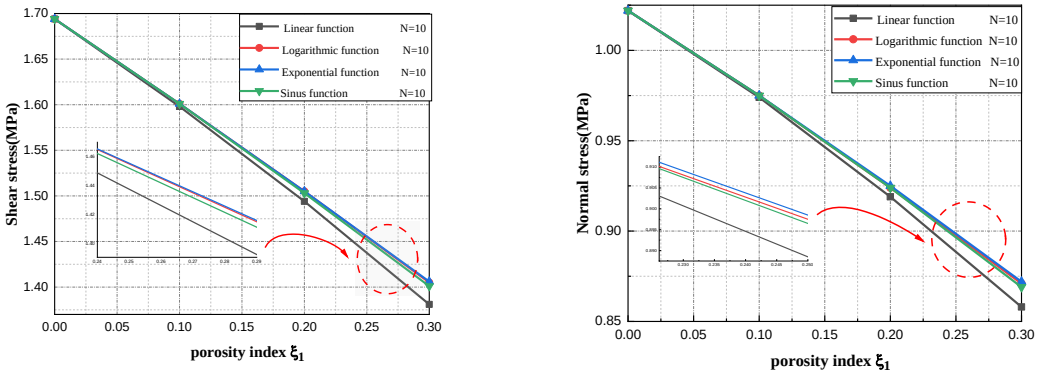

(a) Shear stress (b) Normal stress

Fig. 5 Effect of the porosity on the interfacial stresses of the RC beam strengthened with a porous FGM plate under uniform distributed load

Table 5 Effect of degree homogeneity on interfacial stresses a porous FGM plate under uniform distributed load

Shear stress, P-FGM, $\zeta 1$=0.2				
N	Uneven porosity distribution functions			
	Linear	Logarithmic	exponential	Sinus
0	2.927	2.930	2.930	2.930
2.5	1.972	1.979	1.979	1.978
5	1.702	1.711	1.711	1.710
7.5	1.572	1.581	1.582	1.580
10	1.494	1.505	1.505	1.503
20	1.358	1.36	1.369	1.367
Normal stress, P-FGM, $\zeta 1$=0.2				
N	Uneven porosity distribution functions			
	Linear	Logarithmic	exponential	Sinus
0	1.398	1.399	1.399	1.399
2.5	1.116	1.119	1.119	1.118
5	0.999	1.004	1.004	1.003
7.5	0.947	0.952	0.952	0.952
10	0.919	0.924	0.925	0.924
20	0.877	0.884	0.884	0.883

3.3.2 Effect of degree of homogeneity

Table 5 and Fig. 6 provide the interfacial shear and normal stresses for the RC beam bonded with a porous P-FGM plate where the porosity index ζ_1 equals to 0.2, which demonstrates the effect of plate material properties on interfacial stresses. The length of the plate is L_p = 2400 mm and the thickness of the plate and the adhesive layer are both 4 mm and 2 mm respectively. It can be seen from Table 5 that as the degree of homogeneity increases, both shear and normal stresses decrease.

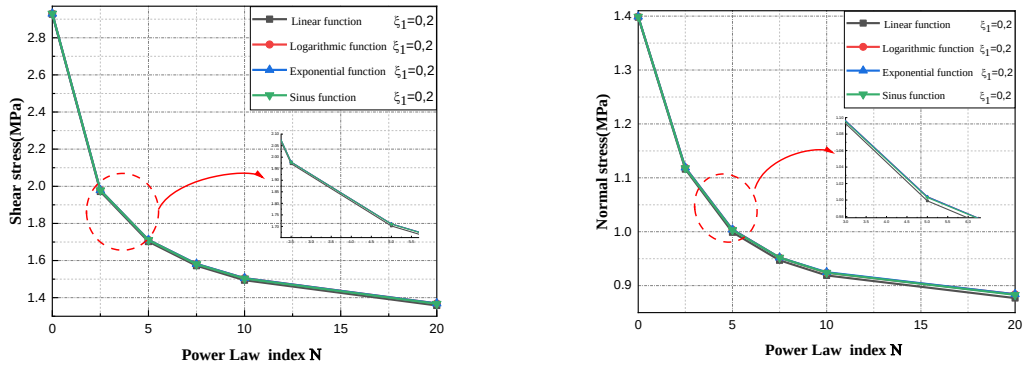

(a) Shear stress (b) Normal stress

Fig. 6 Effect of degree homogeneity on interfacial stresses a porous FGM plate under uniform distributed load

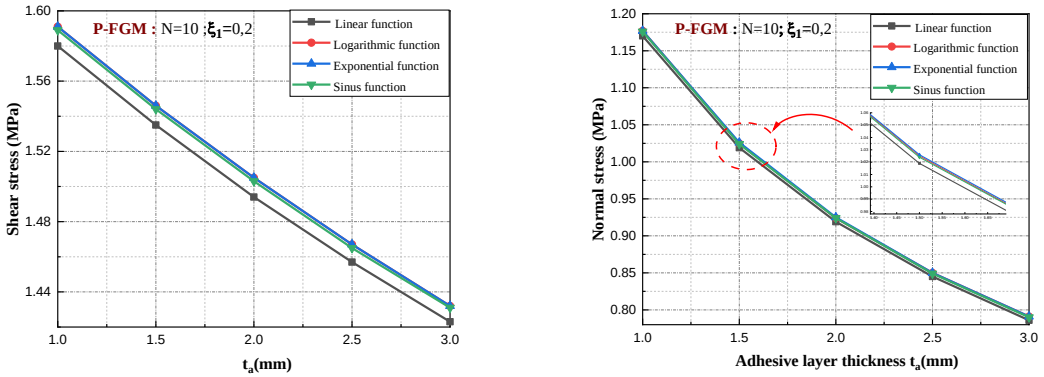

(a) Shear stress (b) Normal stress

Fig. 7 Effect of adhesive layer thickness on edge Interfacial stresses in a porous P-FGM strengthened RC beam under uniform distributed load

3.3.3 Effect of adhesive layer thickness

The effect of the adhesive layer's thickness on the interfacial stresses is shown in the Table 6 and Fig. 7. The interfacial stresses decrease as the thickness of the P-FGM plate increases. Therefore, it is recommended to use a thick adhesive layer, particularly close to the edge.

3.3.4 Effect of the Young's modulus of the adhesive (E_a)

The effect of the Young's modulus of the adhesive on the interfacial stresses of an RC beam strengthened by a porous P-FGM plate is shown in Table 7 and Fig. 8, where the porosity index ζ_1 equals to 0.2 and the degree of homogeneity of the P-FGM is set N = 10. Here, four values of the Young's modulus 3000, 4000, 5000 and 6000 MPa are considered. The thickness of the

Table 6 Effect of adhesive layer thickness on edge Interfacial stresses in a porous P-FGM strengthened RC beam under uniform distributed load

Shear stress, P-FGM, ζ1=0.2				
ta (mm)	Uneven porosity distribution functions			
	Linear	Logarithmic	exponential	Sinus
1	1.580	1.591	1.591	1.589
1.5	1.535	1.546	1.546	1.544
2	1.494	1.505	1.505	1.503
2.5	1.457	1.467	1.467	1.465
3	1.423	1.432	1.432	1.431
Normal stress, P-FGM, ζ1=0.2				
ta (mm)	Uneven porosity distribution functions			
	Linear	Logarithmic	exponential	Sinus
1	1.170	1.177	1.177	1.176
1.5	1.019	1.025	1.026	1.024
2	0.919	0.924	0.925	0.924
2.5	0.845	0.850	0.850	0.849
3	0.786	0.791	0.791	0.790

Table 7 Interfacial stresses of RC beam strengthened with FRP plate for various E_a values under uniform distributed load

Shear stress, P-FGM, ζ1 =0.2, N=10				
E_a (MPa)	Uneven porosity distribution functions			
	Linear	Logarithmic	exponential	Sinus
3000	1.494	1.505	1.505	1.503
4000	1.535	1.545	1.546	1.544
5000	1.561	1.572	1.572	1.570
6000	.580	.590	1.591	1.589
Normal stress, P-FGM, ζ1=0.2, N=10				
Ea(MPa)	Uneven porosity distribution functions			
	Linear	Logarithmic	exponential	Sinus
3000	0.919	0.924	0.925	0.924
4000	1.019	1.025	1.025	1.040
5000	1.101	1.107	1.107	1.106
6000	1.170	1.177	1.177	1.176

adhesive is taken equal to 2 mm. From these results, it can be seen that the interfacial stresses, whether normal or shear stress, increase as the Young's modulus of the adhesive increases.

It can also be observed that the maximum values of the normal and interface shear stresses are obtained for the case of a concrete beam reinforced by a porous FG plate with a pore distribution in exponential form, while the minimum values of the interface constraints are obtained for the case of a porosity distribution in linear form.

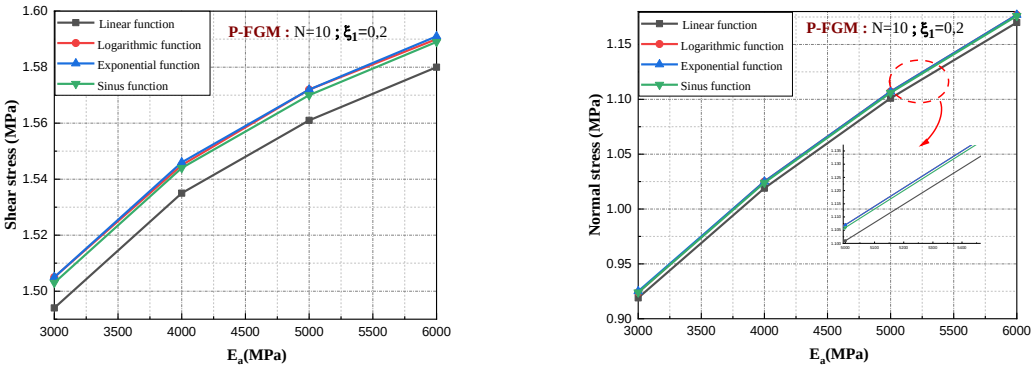

(a) Shear stress (b) Normal stress

Fig. 8 Interfacial stresses of RC beam strengthened with FRP plate for various E_a values under uniform distributed load

Table 8 Influence of length of unstrengthened region on edge stresses for RC beam with a bonded P-FGM soffit plate under uniform distributed load

Shear stress, P-FGM, ζ1 =0.2, N=10				
a(mm)	Uneven porosity distribution functions			
	Linear	Logarithmic	exponential	Sinus
50	0.451	0.455	0.455	0.454
100	0.676	0.681	0.681	0.680
200	1.101	1.109	1.109	1.108
300	1.494	1.505	1.505	1.503
Normal stress, P-FGM, ζ1 =0.2, N=10				
a(mm)	Uneven porosity distribution functions			
	Linear	Logarithmic	exponential	Sinus
50	0.279	0.281	0.281	0.281
100	0.417	0.420	0.420	0.420
200	0.678	0.682	0.682	0.682
300	0.919	0.924	0.925	0.924

3.3.5 Effect of length of unstrengthened region "a"

The normal and shear stresses of an RC beam reinforced in the bending with a porous P-FGM plate are shown in Table 8 and figure 9 effect of the distance of the support at the end of the plate (a). The support's distance from the plate's end is equal. (50, 100, 200 and 300 mm). It is assumed that the thickness of the reinforcing plate is (t_2 = 4 mm). It should be observed that when the distance between the support at the plate's end increases, the interfacial stress becomes more significant.

3.3.6 Effect of plate thickness (t_2)

Fig. 10 and Table 9 give the interfacial normal and shear stresses for the RC beam bonded with a porous P-FGM plate, which demonstrates the effect of plate thickness on the interfacial stresses.

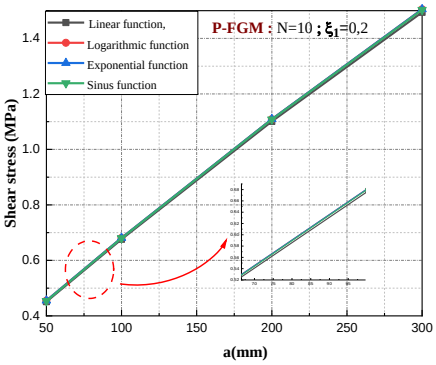

(a) Shear stress

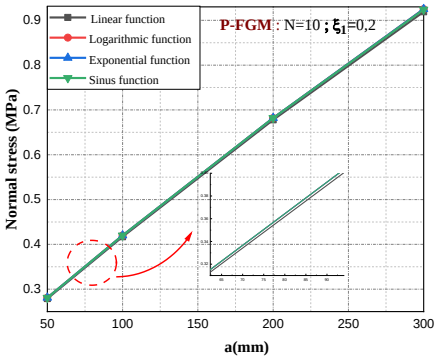

(b) Normal stress

Fig. 9 Influence of length of unstrengthened region on edge stresses for RC beam with a bonded P-FGM soffit plate under uniform distributed load

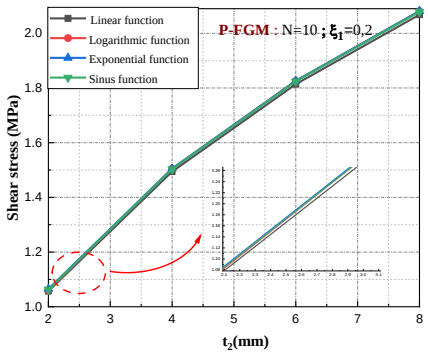

(a) Shear stress

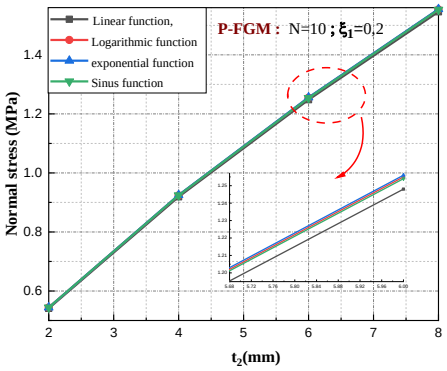

(b) Normal stress

Fig. 10 Effect of the plate thickness on the interfacial stresses of the RC beam strengthened with a porous P-FGM plate under uniform distributed load.

At this time, we changed the thickness of the plate from 2 mm to 8 mm in parallel, the distribution functions of porosity in the P-FGM plate were also tested (Linear function, Logarithmic function, exponential function and Sinus function). It is shown that the level and concentration of interfacial stress are influenced considerably by the thickness of the P-FGM plate. The interfacial stresses increase as the thickness of the P-FGM plate increases.

5. Conclusions

In this study we proposed a new analytical model making it possible to predict the interfacial stresses of a reinforced concrete beam reinforced by a functionally graded plate (FGM) and

Table 9 Effect of the plate thickness on the interfacial stresses of the RC beam strengthened with a porous P-FGM plate under uniform distributed load

Shear stress, P-FGM, $\zeta 1$ =0.2, N=10				
t_2(mm)	Uneven porosity distribution functions			
	Linear	Logarithmic	exponential	Sinus
2	1.057	1.064	1.065	1.063
4	1.494	1.505	1.505	1.503
6	1.814	1.826	1.826	1.824
8	2.068	2.081	2.081	2.079
Normal stress, P-FGM, $\zeta 1$ =0.2, N=10				
t_2(mm)	Uneven porosity distribution functions			
	Linear	Logarithmic	exponential	Sinus
2	0.541	0.544	0.544	0.544
4	0.919	0.924	0.925	0.924
6	1.248	1.255	1.256	1.254
8	1.546	1.554	1.555	1.553

subjected to bending loading. It is also demonstrated the impact of porosity that can occur inside FGM materials during their manufacture. New mixing rules were used taking into account the different porosity distribution rates in the FG plates. To validate this model, we compared the results of the proposed model with those from the literature. The results obtained showed excellent agreement. Additionally, in-depth parametric studies were presented using the proposed solution for reinforced RC beams with different ratios of design parameters. The study of interracial stresses and the factors affecting them provides the basis for understanding delamination failure in such beams and for developing appropriate design rules. The results indicate that there is a considerable concentration of peeling and shear stress at the ends of the FRP plate as compared to the existing solutions. The results show that the normal and shear stresses at the interface are influenced by the material and geometry parameters of the reinforced beam, and that the inhomogeneity's of the reinforcement plate play an important role in the interfacial stress distribution. Observations were made based on the numerical results regarding their possible implications for practical designs. We can conclude that this research is useful for understanding the mechanical behavior of the interface and the design of Concrete-FGM hybrid beams. The current solution is general and can be used with all kinds of materials, unlike traditional solutions.
The present study remains the field of application on reinforced concrete beams with simple supports, and reinforced by FRP plates. So our objective as a continuation of this work in the future is to study the cases of steel or FGM beams reinforced with FRP plates, to introduce the effect of the different types of supports of the beams, to develop a model digital using modeling software such as ANSYS, to introduce the effect of thermal environment and mobile external loads.

References

Abderezak, R., Daouadji, T.H. and Rabia, B. (2021), "Modeling and analysis of the imperfect FGM-damaged RC hybrid beams", *Adv. Comput. Design*, **6**(2), 117-133. https://doi.org/10.12989/acd.2021.6.2.117.

Ait Atmane, R., Mahmoudi, N. and Bennai, R. (2021), "Investigation on the dynamic response of porous

FGM beams resting on variable foundation using a new higher order shear deformation theory", *Steel Compos. Struct.*, **39**(1), 95-107. https://doi.org/10.12989/scs.2021.39.1.095.

Ameur, M., Tounsi, A., Benyoucef, S., Bachir Bouiadjra, M. and Adda Bedia, E. (2009), "Stress analysis of steel beams strengthened with a bonded hygrothermal aged composite plate", *Int. J. Mech. Mater. Design*, **5**, 143-156. https://doi.org/10.1007/s10999-008-9090-2.

Al-Bukhaiti, K., Yanhui, L., Shichun, Z. and Daguang, H. (2024), "Based on BP neural network: Prediction of interface bond strength between CFRP layers and reinforced concrete", *Practice Periodical on Structural Design and Construction*, **29**(2), 04023067. https://doi.org/10.1061/PPSCFX.SCENG-142.

Aslam, M., Shafigh, P., Jumaat, M.Z. and Shah, S. (2015), "Strengthening of RC beams using prestressed fiber reinforced polymers–A review", *Constr. Build. Materi.*, 82, 235-256. https://doi.org/10.1016/j.conbuildmat.2015.02.051.

Ayache, B., Bennai, R., Fahsi, B., Fourn, H., Atmane, H.A. and Tounsi, A. (2018), "Analysis of wave propagation and free vibration of functionally graded porous material beam with a novel four variable refined theory", *Earthq. Struct.*. **15**(4), 369-382. https://doi.org/10.12989/eas.2018.15.4.369.

Bai, Y.L., Niu, W.Q., Xie, W.J. and Gao, W.Y. (2024), "Flexural behavior of reinforced concrete beams strengthened with hybrid carbon FRP laminates", *Constr. Build. Mater.*, **411**, 2024, 134372. https://doi.org/10.1016/j.conbuildmat.2023.134372.

Benachour, A., Benyoucef, S. and Tounsi, A. (2008), "Interfacial stress analysis of steel beams reinforced with bonded prestressed FRP plate", *Eng. Struct.*, **30**(11), 3305-3315. https://doi.org/10.1016/j.engstruct.2008.05.007.

Bennai, R., Atmane, H.A., Ayache, B., Tounsi, A., Bedia, E.A. and Al-Osta, M. (2019), "Free vibration response of functionally graded Porous plates using a higher-order Shear and normal deformation theory", *Earthq. Struct.*, **16**(5), 547-561. https://doi.org/10.12989/eas.2019.16.5.547.

Bennai, R., Fourn, H., Atmane, H.A., Tounsi, A. and Bessaim, A. (2019), "Dynamic and wave propagation investigation of FGM plates with porosities using a four variable plate theory", *Wind Struct.*, **28**(1), 49-62. https://doi.org/10.12989/was.2019.28.1.049.

Bennai, R., Atmane, R. A., Bernard, F., Nebab, M., Mahmoudi, N., Atmane, H.A. and Tounsi, A. (2022), "Study on stability and free vibration behavior of porous FGM beams", *Steel Compos. Struct.*, **45**(1), 67-82. https://doi.org/10.12989/scs.2022.45.1.067.

Benyoucef, S., Tounsi, A., Yeghnem, R., Bachir Bouiadjra, M. and Adda Bedia, E. (2014), "An analysis of interfacial stresses in steel beams bonded with a thin composite plate under thermomechanical loading", *Mech. Compos. Mater.*, **49**, 641-650. https://doi.org/10.1007/s11029-013-9380-0.

Berradia, M., Azab, M., Ahmad, Z., Accouche, O., Raza, A. and Alashker, Y. (2022), "Data-driven prediction of compressive strength of FRP-confined concrete members: An application of machine learning models", *Struct. Eng. Mech.*, **83**(4), 515-535. https://doi.org/10.12989/sem.2022.83.4.515.

Bouakaz, K., Daouadji, T.H., Meftah, S., Ameur, M., Tounsi, A. and Bedia, E.A. (2014), "A numerical analysis of steel beams strengthened with composite materials", *Mech. Compos. Mater.*, **50**, 491-500. https://doi.org/10.1007/s11029-014-9435-x.

Bouchikhi, A., Megueni, A., Gouasmi, S. and Boukoulda, F. (2013), "Effect of mixed adhesive joints and tapered plate on stresses in retrofitted beams bonded with a fiber-reinforced polymer plate", *Mater. Design*, **50**, 893-904. https://doi.org/10.1016/j.matdes.2013.03.052.

Daouadji, H.T., Benyoucef, S., Tounsi, A., Benrahou, K. and Bedia, A.E. (2008), "Interfacial stress concentrations in FRP-damaged RC hybrid beams", *Compos. Interfaces*, **15**(4), 425-440. https://doi.org/10.1163/156855408784514702

Daouadji, T.H. (2013), "Analytical analysis of the interfacial stress in damaged reinforced concrete beams strengthened by bonded composite plates", *Strength of Materials*. **45**(5), 587-597. https://doi.org/10.1007/s11223-013-9496-4.

Daouadji, T.H., Chedad, A. and Adim, B. (2016), "Interfacial stresses in RC beam bonded with a functionally graded material plate", *Struct. Eng. Mech.*, **60**(4), 693-705. https://doi.org/10.12989/sem.2016.60.4.693.

Daouadji, T.H., Rabahi, A., Abbes, B. and Adim, B. (2016), "Theoretical and finite element studies of

interfacial stresses in reinforced concrete beams strengthened by externally FRP laminates plate", *J. Adhesion Sci. Technol*., **30**(12), 1253-1280. https://doi.org/10.1080/01694243.2016.1140703.

Du, Y.X., Hou, C.X., Xu, B. and Zhou, F. (2016), "Effect of shear deformation on interfacial stress of fiber-reinforced polymer plate–strengthened reinforced concrete beams", *Adv. Struct. Eng.*. **19**(10), 1592-1603. https://doi.org/10.1177/1369433216645990.

Du, Y., Liu, Y. and Zhou, F. (2019), "An improved four-parameter model on stress analysis of adhesive layer in plated beam", *Int. J. Adhesion Adhesives*, **91**, 1-11. https://doi.org/10.1016/j.ijadhadh.2019.02.005.

Fahsi, B., Benrahou, K.H., Krour, B., Tounsi, A., Benyoucef, S. and Adda Bedia, E.A. (2011), "Analytical analysis of interfacial stresses in FRP-RC hybrid beams with time-dependent deformations of RC beam", *Acta Mechanica Solida Sinica*, **24**(6), 519-526. https://doi.org/10.1016/S0894-9166(11)60052-9.

Farouk, M.A., Moubarak, A.M.R. and Ibrahim, A. (2023), "New alternative techniques for strengthening deep beams with circular and rectangular openings", *Case Studies Constr. Mater*., **19**, e02288, https://doi.org/10.1016/j.cscm.2023.e02288.

Guenaneche, B. and Tounsi, A. (2014), "Effect of shear deformation on interfacial stress analysis in plated beams under arbitrary loading", *Int. J. Adhesion Adhesives*, **48**, 1-13. https://doi.org/10.1016/j.ijadhadh.2013.09.016.

Gupta, A. and Talha, M. (2017), "Influence of porosity on the flexural and vibration response of gradient plate using nonpolynomial higher-order shear and normal deformation theory", *Int. J. Mech. Mater. Design*, **14**(2), 277-296. https://doi.org/10.1007/s10999-017-9369-2.

Hamoda, A.A., Eltaly, B.A., Ghalla, M. and Liang, Q.Q. (2023), "Behavior of reinforced concrete ring beams strengthened with sustainable materials", *Eng. Struct.*, **290**, 116374. https://doi.org/10.1016/j.engstruct.2023.116374.

He, X., Zhou, C., Lv, M., Wang, Y. and Liu, Y. (2023), " Interfacial stresses of beams hybrid strengthened by steel plate with outside taper and FRP pocket", *J. Build. Eng.*, 107034. https://doi.org/10.1016/j.jobe.2023.107034.

Kim, E.J., Lee, C.M. and Kim, D.H. (2023), "Study on the characteristics of functionally graded materials from Ni-20cr to Ti-6Al-4V via directed energy deposition", *J. Alloys Compounds*, **955** 170263. https://doi.org/10.1016/j.jallcom.2023.170263.

Krour, B., Bernard, F. and Tounsi, A. (2013), "Fibers orientation optimization for concrete beam strengthened with a CFRP bonded plate: A coupled analytical–numerical investigation", *Eng. Struct*., **56**, 218-227. https://doi.org/10.1016/j.engstruct.2013.05.008.

Liu, M. and Dawood, M. (2018), "A closed-form solution of the interfacial stresses and strains in steel beams strengthened with externally bonded plates using ductile adhesives", *Eng. Struct*., **154**, 66-77. https://doi.org/10.1016/j.engstruct.2017.10.054.

Long, H., Wei, Y. and Liang, L. (2020), "A rigorous analytical solution of interfacial stresses and overall stiffness of beam structures bonded with partially covered plates", *Int. J. Mech. Sci*., **167**, 105284. https://doi.org/10.1016/j.ijmecsci.2019.105284.

Mellal, F., Bennai, R., Nebab, M., Atmane, H.A., Bourada, F., Hussain, M. and Tounsi, A. (2021), "Investigation on the effect of porosity on wave propagation in FGM plates resting on elastic foundations via a quasi-3D HSDT", *Waves Random Complex Media*, 1-27. https://doi.org/10.1080/17455030.2021.1983235.

Mellal, F., Bennai, R., Avcar, M., Nebab, M. and Atmane, H.A. (2023), "On the vibration and buckling behaviors of porous FG beams resting on variable elastic foundation utilizing higher-order shear deformation theory", *Acta Mech*., **234**, 3955-3977. https://doi.org/10.1007/s00707-023-03603-5.

Mohamed, B.B., Abdelouahed, T., Samir, B. and El Abbas, A.B. (2009), "Approximate analysis of adhesive stresses in the adhesive layer of plated RC beams", *Comput. Mater. Sci.*, **46**(1), 15-20. https://doi.org/10.1016/j.commatsci.2009.01.020.

Nebab, M., Atmane, H.A., Bennai, R., Tounsi, A. and Bedia, E.A. (2019), "Vibration response and wave propagation in FG plates resting on elastic foundations using HSDT", *Struct. Eng. Mech*., **69**(5), 511-525. https://doi.org/10.12989/sem.2019.69.5.511.

Rabahi, A., Benferhat, R., Daouadji, T.H., Abbes, B., Belkacem, A. and Abbes, F. (2018), "Elastic analysis of interfacial stresses in prestressed PFGM-RC hybrid beams", *Adv. Mater. Res.*, **7**(2), 83.

https://doi.org/10.12989/amr.2018.7.2.083.
Rabahi, A., Daouadji, T.H., Abbes, B. and Adim, B. (2016), "Analytical and numerical solution of the interfacial stress in reinforced-concrete beams reinforced with bonded prestressed composite plate", *J. Reinforc. Plast. Compos.*, **35**(3), 258-272. https://doi.org/10.1177/0731684415613633.
Rabia, B., Abderezak, R., Daouadji, T.H., Abbes, B., Belkacem, A. and Abbes, F. (2018), "Analytical analysis of the interfacial shear stress in RC beams strengthened with prestressed exponentially-varying properties plate", *Adv. Mater. Res.*, **7**(1), 29-44. https://doi.org/10.12989/amr.2018.7.1.029.
Rabia, B., Daouadji, T.H. and Abderezak, R. (2020), "Predictions of the maximum plate end stresses of imperfect FRP strengthened RC beams: study and analysis", *Adv. Mater. Res.*, **9**(4), 265-287. https://doi.org/10.12989/amr.2020.9.4.265.
Raza, A., Alomayri, T. and Berradia, M. (2022), "Rapid repair of partially damaged GFRP-reinforced recycled aggregate concrete columns using FRP composites", *Mech. Adv. Mater. Struct.*, **29**(27), 6070-6086. https://doi.org/10.1080/15376494.2021.1972368.
Sami, A., Khan, Q.Z., Azam, A., Raza, A. and Berradia, M. (2022), "Performance of repaired macro-synthetic structural fibers and glass-FRP-reinforced concrete columns", *Iran. J. Sci. Technol. Trans. Civil Eng.*, 1-12. https://doi.org/ 10.1007/s40996022-00966-y.
Sha, X. and Davidson, J.S. (2020), "Analysis of interfacial stresses in concrete beams strengthened by externally bonded FRP laminates using composite beam theory", *Compos. Struct.*, **243**, 112235. https://doi.org/10.1016/j.compstruct.2020.112235.
Shan, Z. and Su, R. (2020), "Improved uncoupled closed-form solution for adhesive stresses in plated beams based on Timoshenko beam theory", *Int. J. Adhesion Adhesives*, **96**, 102472. https://doi.org/10.1016/j.ijadhadh.2019.102472.
Smith, S.T. and Teng, J. (2001), "Interfacial stresses in plated beams", *Eng. Struct.*, **23**(7), 857-871. https://doi.org/10.1016/S0141-0296(00)00090-0.
Teng, J., Zhang, J. and Smith, S.T. (2002), "Interfacial stresses in reinforced concrete beams bonded with a soffit plate: a finite element study", *Constr. Build. Mater.*, **16**(1), 1-14. https://doi.org/10.1016/S0950-0618(01)00029-0.
Tounsi, A. (2006), "Improved theoretical solution for interfacial stresses in concrete beams strengthened with FRP plate", *Int. J. Solids Struct.*, **43**(14-15), 4154-4174. https://doi.org/10.1016/j.ijsolstr.2005.03.074.
Tounsi, A. and Benyoucef, S. (2007), "Interfacial stresses in externally FRP-plated concrete beams", *Int. J. Adhesion Adhesives*, **27**(3), 207-215. https://doi.org/10.1016/j.ijadhadh.2006.01.009.
Van Pham, P. (2021), "Solutions of the interfacial shear and normal stresses in plate flexural-strengthened beams based on different complementary strain energy assumptions", *Eng. Struct.*, **229**, 111567. https://doi.org/10.1016/j.engstruct.2020.111567.
Wang, Y.Q., Wan, Y.H. and Zhang, Y.F. (2017), "Vibrations of longitudinally traveling functionally graded material plates with porosities", *Eur. J. Mech. - A/Solids*. **66**, 55-68. https://doi.org/10.1016/j.euromechsol.2017.06.006.
Wattanasakulpong, N. and Ungbhakorn, V. (2014), "Linear and nonlinear vibration analysis of elastically restrained ends FGM beams with porosities", *Aerosp. Sci. Technol.*, **32**(1), 111-120. https://doi.org/10.1016/j.ast.2013.12.002.
Yang, J., Chen, J.F. and Teng, J. (2009), "Interfacial stress analysis of plated beams under symmetric mechanical and thermal loading", *Constr. Build. Mater.*, **23**(9), 2973-2987. https://doi.org/10.1016/j.conbuildmat.2009.05.004.
Zhang, E., Zhang, J., Chen, B., Liu, C. and Zhan, Y. (2023), "Finite element analysis of laser ultrasonic in functionally graded material", *Appl. Acoustics*, **204**, 109243. https://doi.org/10.1016/j.apacoust.2023.109243.
Zhang, L. and Teng, J. (2010), "Finite element prediction of interfacial stresses in structural members bonded with a thin plate", *Eng. Struct.*, **32**(2), 459-471. https://doi.org/10.1016/j.engstruct.2009.10.008.